LA-UR-19-29161
Approved for public release; distribution is unlimited.

Title: High Dose Irradiation of Austenitic Alloys

Author(s): Gigax, Jonathan Gregory
Kim, Hyosim
Li, Nan

Intended for: Report

Issued: 2019-09-12

High Dose Irradiation of Austenitic Alloys

Fuel Cycle Research & Development

Prepared for
U.S. Department of Energy
Advanced Fuels Campaign

Jonathan G. Gigax
Hyosim Kim
Nan Li

08/29/19

SUMMARY

The present report provides a short summary of our recent efforts to irradiate an austenitic iron alloy, D9, and a face-center cubic high entropy alloy (HEA) to a damage level of 400 peak dpa. The irradiated microstructure of D9 showed little void swelling and the presence of a large density of carbides in the irradiated region. This indicated a potential issue either with the irradiation environment (i.e. chamber contamination) or specimen preparation. The HEA examined showed very little swelling in the matrix and possibly no carbides. Further examination of the microstructure revealed the formation of numerous precipitates that are coherent with the matrix based on diffraction pattern analysis. In this temperature range, the lack of swelling and formation of these precipitates indicates the superior radiation resistance of this HEA alloy.

TABLE OF CONTENTS

FIGURES

TABLES

Intentionally Blank

1. Introduction

2. Materials and Methods

D9 was fabricated by Carpenter Technologies with a composition given in Table 1. An equiatomic FeCrNiMn high entropy alloy (HEA) was fabricated by Sophisticated Alloys Inc. The HEA was cast and consolidated by a hot isostatic press at a pressure of 100 MPa and at 1200 °C. Specimens were cut into roughly 5 mm x 5 mm specimens, ground to 0.75 mm thickness, and polished to a final solution of 0.04 um silica. The samples were irradiated with 3.5 MeV Fe ions at the Texas A&M University Radiation Materials Characterization Laboratory and Facility using a 3 MV NEC pelletron. The D9 and HEA was irradiated at a temperature of 575 °C to damage levels of 100, 200, 300, and 400 peak dpa. Damage levels were calculated using the SRIM-2013 software package and a displacement energy of 40 eV [3,4]. A static, defocused beam was used to avoid the influence of rastering on void swelling [5]. Cryotraps and a magnetic filtering magnet were used to remove contaminants from the beam line and chamber in an effort to avoid composition modification by carbon injection [6]. Due to the long duration of the ion irradiation and limited time available for analysis, only the 400 peak dpa specimens were analyzed.

Table 1. Chemical composition of the D9 and HEA alloy

Alloy ID	Fe	Cr	Ni	Mn	Mo	Si	Ti	Ta	Al	P	S	C	N	O
D9	Bal.	13.53	15.56	2.11	1.65	0.85	0.3	0.01	0.004	0.002	0.005	0.034	0.0017	0.0012
HEA	25	25	25	25										

A FEI Helios focused ion beam mill (FIB) was used to perform conventional cross-section lamella lift-out and thinning for transmission electron microscopy (TEM). After thinning the specimen to a thickness less than 100 nm, the micrographs of the lamella were obtained on a FEI Tecnai F30 operated at 300 kV via conventional bright field, dark field, and scanning transmission electron microscopy (STEM) with a high angle annular dark field detector (HAADF).

3. Results and Discussion

3.1 Microstructure of D9 after 400 peak dpa

Figure 1 provides a brightfield image of the D9 after heavy ion irradiation to 400 peak dpa. From this image, a high density of large precipitates (carbides) are visible. Only one or two voids were observed in the irradiated region. Based on our previous work in two other austenitic alloys, A709 and 316, this dose and temperature should lead to an exceptional amount of swelling (>50%). The microstructure in Fig. 1 suggests that a couple of issues may be present. First, either the specimen or irradiation chamber was contaminated with C-rich molecules. This carbide formation was observed in a ferritic/martensitic alloy, HT9, and was eventually solved by use of different filtering techniques [6]. Even though those filtering techniques were employed in this study, contamination on the sample or in the target chamber would not be completely removed.

Second, the irradiation conditions, namely the sample temperature may not have been at the target temperature in the irradiation. This may be due to either poor thermal contact made by the adhesion material (i.e. silver paste) or an incorrect reading from stage thermal couples. If we assume that void swelling in austenitic materials should persist even with carbon injection, then the lack of void swelling indicates that the specimen may not have been at the correct temperature. Regardless of the reason, the current result is not to expectations and any investigation on the other D9 specimens will be paused until new irradiations can be performed with voids apparent in the material.

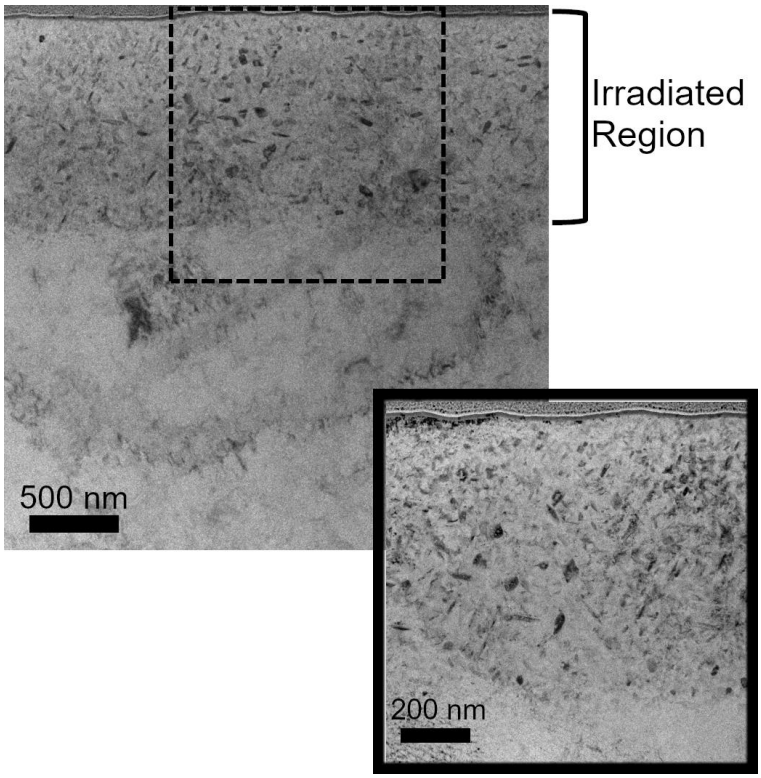

Figure 1 – Brightfield micrograph of the D9 irradiated to 400 peak dpa. Inset image shows a higher magnification area in the irradiated region.

3.2 Microstructure of the HEA after 400 peak dpa

Figure 2 provides overview brightfield and darkfield micrographs for the HEA irradiated to 400 peak dpa. Numerous precipitates in the near surface region are observed, in addition to minor oxidation on the surface of the specimen. The darkfield image in Fig. 2a provides a little bit more clarity to distinguish the precipitates from other features. The darkfield image was taken by selecting one reflection belonging to the precipitates with an objective aperture.

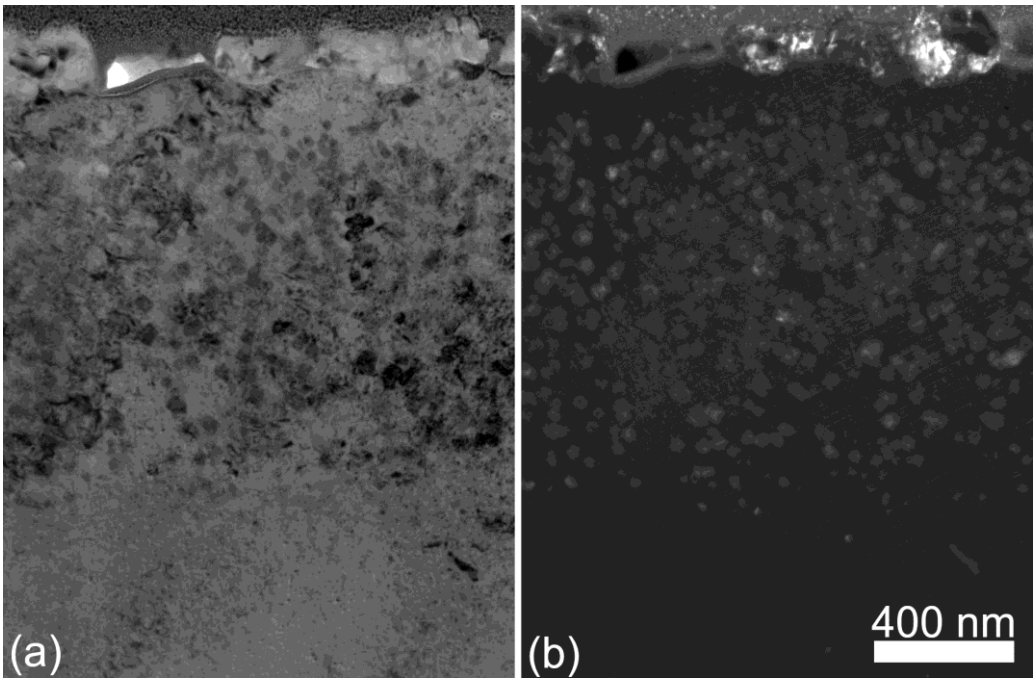

Figure 2 – (a) Brightfield and (b) darkfield TEM micrographs of INL HT9 irradiated to 600 peak dpa.

Fig. 3 shows diffraction patterns taken from the HEA at the $[11\bar{2}]$ zone axis in the irradiated and unirradiated region, respectively. Here, a superlattice is easily observed in the near surface region taking on the same pattern as the matrix. A white circle in Fig 3b denotes the location of the aperture in darkfield imaging in Fig. 2. Outside of the irradiated region, no superlattice is observed, indicating that the precipitates are radiation-induced. Furthermore, these precipitates are likely comprised of the constituents of the matrix (i.e. Fe, Cr, Mn, Ni) since carbides and oxides of these materials are not likely to be coherent with the matrix.

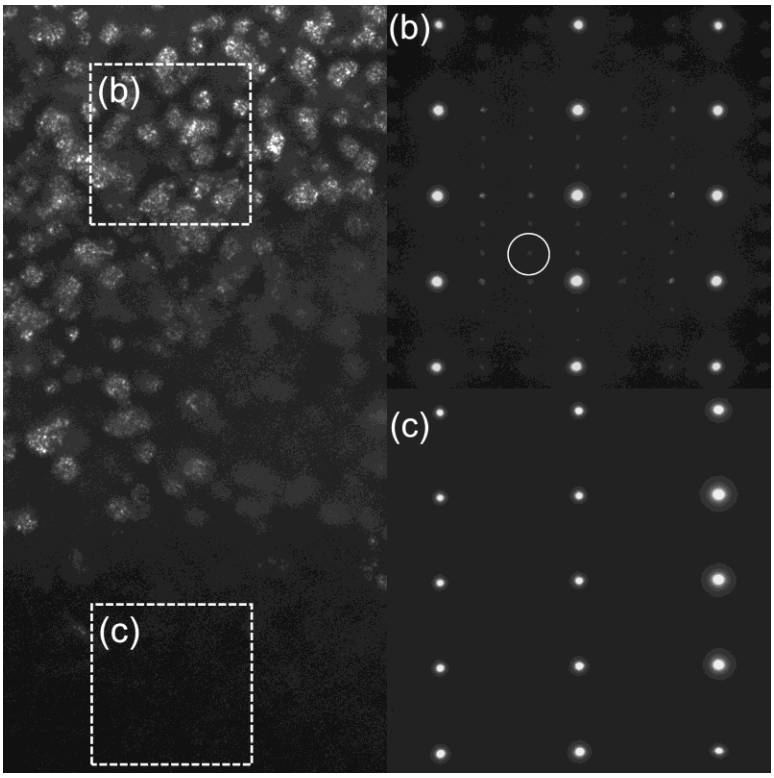

Figure 3 – (a) Darkfield micrograph of the HEA irradiated to 400 peak dpa. Selected area diffraction pattern taken from the (a) irradiated and (b) unirradiated regions.

Fig. 4 provides a higher magnification image of the precipitates. Clearly, there is some internal structure in each that does not appear bright (i.e. coherent). With our current analysis, it is difficult to conclude what those particular features are. In one precipitate, the feature is a void. However, there is another possibility that these are other precipitates as well. In darkfield imaging, incoherent particles or voids would not appear bright and do not conclusively identify the particles in question.

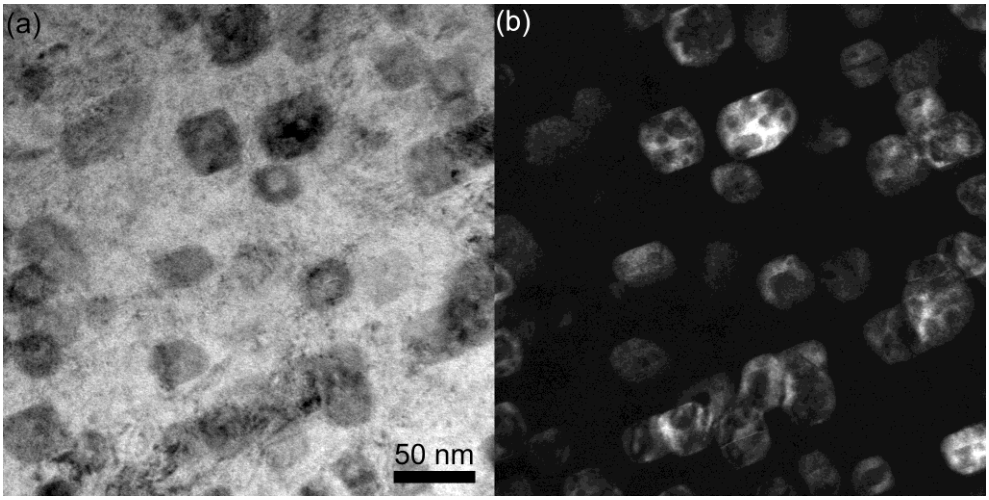

Figure 4 – (a) Brightfield and (b) darkfield micrographs at a higher magnification in the irradiated region of the HEA irradiated to 400 peak dpa. The scale bar in (a) applies to both images.

4. Conclusions and Future Work

In this study, we performed heavy ion irradiation of a D9 and HEA alloy up to a damage level of 400 peak dpa. The D9 examined showed numerous carbides in the irradiated region, suggesting that contamination was present during the irradiation. The lack of void swelling may be caused by carbide formation and other factors as well.

The HEA showed the formation of large (50 nm) precipitates in the near surface region after ion irradiation. These particles were found to be coherent with the matrix from diffraction patterns. A closer examination of these at a higher resolution showed that the particles have some internal structure with what appear to be either voids or incoherent particles present.

At this stage, before investing additional time into either sample set, our plan is to perform the irradiation under cleaner conditions. Our expectation is that the D9 should swell at 400 peak dpa, similar to what we observed in 316. If this is observed, we will also verify that the microstructure of the HEA after irradiation remains unchanged. Additional analysis, including elemental maps will be made to understand the changes to the microstructure of the HEA after irradiation.

5. References

1. M.B. Toloczko, F. A Garner, C. R. Eiholzer, Irradiation creep and swelling of US fusion heats of HT9 and 9Cr-1Mo to 208 dpa at ~400 C, J. Nucl. Mater. 212-215 (1994) 604-607.
2. M.B. Toloczko and F. A Garner, Irradiation creep and void swelling of two LMR heats of HT9 at~400°C and 165dpa, J. Nucl. Mater. 233-237 (1996) 289-292.
3. J.F. Ziegler, M.D. Ziegler, J.P. Biersack, SRIM: The stopping and range of ions in matter, Nucl. Instr. Methods Phys. Res. B 268 (2010).
4. R. Stoller, M.B. Toloczko, G.S. Was, A.G. Certain, S. Dwaraknath, F.A. Garner, On the use of SRIM for computing radiation damage exposure, Nucl. Methods Phys. Res. Sect. B 310 (2013) 75-80.
5. J. G. Gigax, E. Aydogan, T. Chen, D. Chen, L. Shao, Y. Wu, W. Y. Lo, Y. Yang, and F. A. Garner, The influence of ion beam rastering on the swelling of self-ion irradiated pure iron at 450°C, J. Nucl. Mater. 465 (2015) 343–348.
6. J. G. Gigax, H. Kim, E. Aydogan, F. A. Garner, S. A Maloy, and L. Shao, Beam-contamination-induced compositional alteration and its neutron-atypical consequences in ion simulation of neutron-induced void swelling, Mater. Res. Lett. 5 (2017) 478-485.
7. J. G. Gigax, T. Chen, H. Kim, J. Wang, L. M. Price, E. Aydogan, S. A. Maloy, D. K. Schreiber, M. B. Toloczko, F. A. Garner, and Lin Shao, Radiation response of alloy T91 at damage levels up to 1000 peak dpa, J. Nucl. Mater. 482 (2016) 257-265.
8. J. G. Gigax, H. Kim, T. Chen, F. A. Garner, and L. Shao, Radiation instability of equal channel angular extruded T91 at ultra-high damage levels, Acta Mater. 132 (2017) 395-404.
9. L. Shao, C-C. Wei, J. G. Gigax, A.Aitkaliyeva, D. Chen, B. H. Sencer, and F. A. Garner, Effect of defect imbalance on void swelling distributions produced in pure iron by 3.5 MeV self-ions, J. Nucl. Mater. 453 (2014) 176–181.